IEEE Photonics Journal
An IEEE Photonics Society Publication

Open Access

An Augmented-Reality Device With Switchable Integrated Spaces Using a Bi-Focal Integral Floating Display

Volume 11, Number 4, August 2019

Minyoung Park
Kyung-Il Joo
Hak-Rin Kim
Hee-Jin Choi

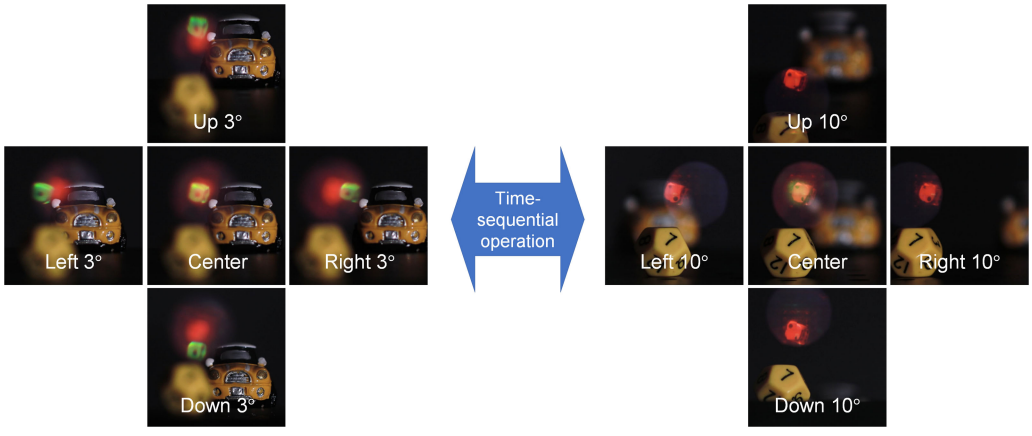

DOI: 10.1109/JPHOT.2019.2924688

An Augmented-Reality Device With Switchable Integrated Spaces Using a Bi-Focal Integral Floating Display

Minyoung Park,[1] **Kyung-Il Joo**,[2] **Hak-Rin Kim**,[2] **and Hee-Jin Choi** [1]

[1]Department of Physics, Sejong University, Seoul 05006, South Korea
[2]School of Electronics Engineering, Kyungpook National University, Daegu 41566, South Korea

DOI:10.1109/JPHOT.2019.2924688

Manuscript received June 3, 2019; revised June 16, 2019; accepted June 19, 2019. Date of publication June 24, 2019; date of current version August 2, 2019. This work was supported in part by the Technology Innovation Industrial Program funded by the Ministry of Trade, Industry and Energy (MI, Korea) under Program 10052667—Development of high sensitive (<30 mJ/cm2) R/G/B color photo-rewritable 3D holographic materials and 1 fps speed frame switching technology—and in part by the Basic Science Research Program through the National Research Foundation of Korea funded by the Ministry of Education (2018R1D1A1B07049563). This paper has supplementary downloadable material available at http://ieeexplore.ieee.org. *(Minyoung Park and Kyung-Il Joo contributed equally to this work.)*
Corresponding author: Hee-Jin Choi (e-mail: hjchoi@sejong.ac.kr).

Abstract: An augmented-reality (AR) device which presents virtual volumetric images to switchable integrated spaces is proposed and demonstrated. A bi-focal geometric phase (GP) lens can project the integrated volumetric images to switchable integrated spaces by switching the polarization of them. For that purpose, a combination of GP lens and an active polarization switching device has been adopted. A demonstration of an AR display with switchable integrations is also provided to verify the proposed concept.

Index Terms: Augmented-reality, switchable integrated spaces, integral imaging.

1. Introduction

The AR display presenting virtual images on a real-world scene is thought to be one of the promising immersive devices for various field such as education, automobile, and manufacturing. However, even the latest ones of commercial AR devices at the state of the art are able to project only a single planar image plane at a fixed distance. In order to resolve that problem, researchers in the field have proposed methods to provide more realistic AR images by realizing volumetric AR devices based on the principles of holography [1], [2], integral imaging [3], [4], and multi-focal-planes [5]–[8]. Nevertheless, there still exist some bottlenecks that the holography method suffers from narrow viewing angle, integral imaging approaches are having limited expression of three-dimensional (3D) depth, and multi-focal-planes display provides multiple planar images, which are not volumetric.

The integral floating display which is composed of a display device, a lens array, and a floating lens has been verified by several analyses that it can enhance the viewing parameters of the volumetric 3D image including the depth expression. Thus, there have been ideas to implement a volumetric AR device using that advantage by adopting a convex half mirror or a freeform prism as variations of a floating lens [9], [10]. However, even the most advanced ideas above are still under the fundamental limitation that the image volume (the depth expression of the volumetric image) is

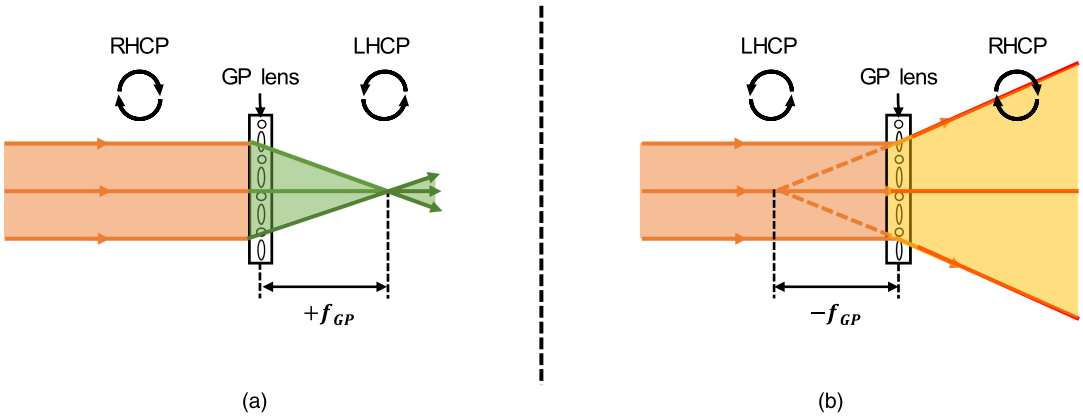

Fig. 1. Dual optical property of GP lens with a focal length of (a) $+f_{GP}$ (convex) and (b) $-f_{GP}$ (concave) dependent on the polarization (RHCP/LHCP) of incident light.

restricted around the image plane of the floating optics. Thus, a novel method to provide expanded image volume is needed for providing a realistic experience to the observer. For that purpose, we proposed an AR device which is expressible switchable integrated spaces to present dual 3D volumetric images using a bi-focal integral floating display synchronized with an active polarization switching device (APSD).

2. Principles

A geometric phase (GP) lens is a device to have bi-focal lengths ($\pm f_{GP}$) switched by the polarization of the incident light [11]. As shown in Fig. 1(a), the GP lens acts like a convex lens with $+f_{GP}$, when incident light has a right-handed circular polarization (RHCP). In contrast, it has a negative focal length of $-f_{GP}$ when polarization-switched incident light has left-handed circular polarization (LHCP), as shown in Fig. 1(b) [12]. Therefore, adopting the GP lens makes the integral floating display have switchable integrated spaces where volumetric AR images are integrated around the bi-focal planes.

The principles of a bi-focal integral floating display are as shown in Fig. 2. The system is using a liquid crystal display (LCD) panel and a lens array to provide 3D volumes with elemental image sets. Then the GP lens acts as a convex or a concave lens to project those 3D volumes to the designated spaces when the APSD modulates the incident light with 45° linear polarization (LP) to have a RHCP or a LHCP states, respectively. With that combination, it is possible to realize switchable integrated spaces in a time-sequential operation as shown in Fig 2.

Besides the formation of the dual image volumes, a synchronization between the displayed images and their polarization is needed for presenting the volumetric images properly. For that purpose, we implemented an APSD to switch the polarization electrically at every refreshment timing of the display images. The APSD has the stacked optical structure of a twisted nematic liquid crystal (TN LC) cell and an achromatic $\lambda/4$ retarder film (#88-251, Edmund optics). The TN LC layer can actively switch the 45° LP light from the LCD panel to 45° LP or to $-45°$ LP, depending on an applied voltage condition. The thickness of the TN LC layer was designed to be 5 μm, which satisfies the 2nd solution condition of the Gooch–Terry equation, so as to minimize the chromatic dispersion effect in obtaining field-switching of two orthogonal LP states [13]. The linearly polarized light passing through the TN LC cell is converted to RHCP or LHCP by the achromatic $\lambda/4$ retarder film. The slow axis of the $\lambda/4$ retarder film is set to the x-axis. Without an applied voltage to the TN LC cell, the 45° LP made by the exit polarizer of the LCD panel is converted into the $-45°$ LP by the polarization rotation effect of the TN LC cell, and the $-45°$ LP from the TN LC is converted into LHCP by the $\lambda/4$ retarder film before the GP lens, as shown in Fig. 3(a). At a field-on state

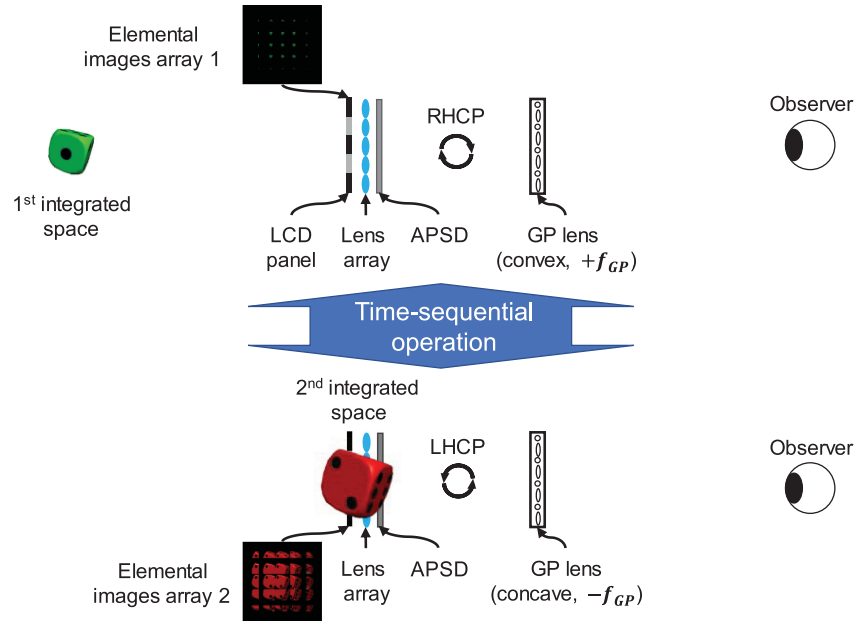

Fig. 2. Structure and principles of the proposed system with a time-sequential displaying of switchable integrated spaces.

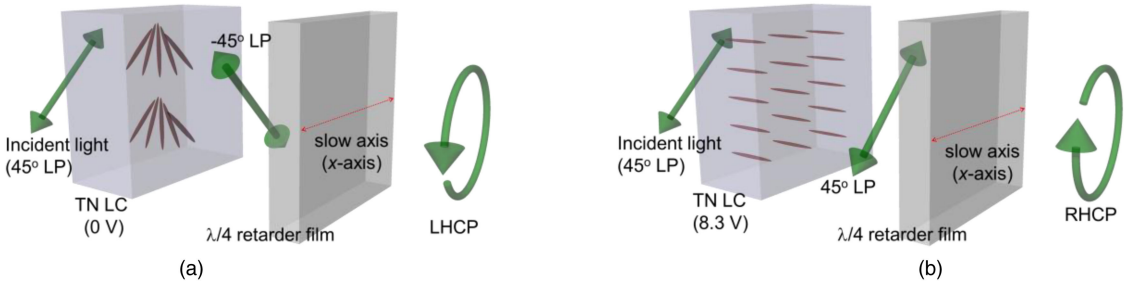

Fig. 3. Structure and principles of the APSD composed of a TN LC cell and an achromatic λ/4 retarder film: (a) field-off state, and (b) field-on state, respectively.

(8.3 V_{pp} at 1 kHz AC operation in our experiment), the TN LC layer is changed into an optical C-plate by the field-induced dielectric torque of the LC molecules. The 45° LP is maintained with the incident polarization state and the 45° LP is converted to RHCP by the λ/4 retarder film, as shown in Fig. 3(b). Therefore, the APSD can actively switch the incident polarization state onto the GP lens between the RHCP and LHCP states according to the applied voltage condition of the TN LC cell.

3. Experiments

3.1 Experimental Setup

With the principles above, we realized an AR display with switchable integrated spaces as shown in Fig. 4. The experimental setup provides two volumetric AR images of a green die and a red die in the 1st and the 2nd integrated spaces, respectively. The LCD panel has a pixel pitch of 47 μm and a refresh rate of 50 Hz. The lens array between the LCD panel and the APSD has a focal length f_{LA} of 10 mm and consists of elemental lenses with pitch of 5 mm. The GP lens used has

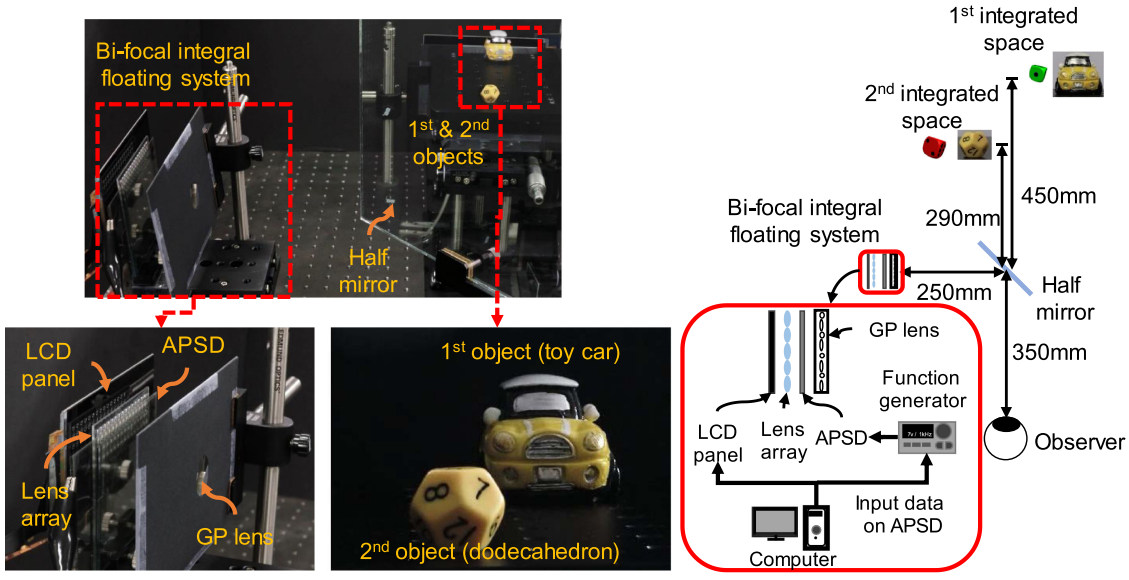

Fig. 4. Experimental setup of a bi-focal integral floating display with dual integrated spaces. The 1st volumetric AR images (green die) and 1st object (toy car) are located 800 mm far from the observer. The 2nd volumetric AR images (red die) and 2nd object (dodecahedron) are at 640 mm from the observer.

bi-focal lengths of ±100 mm. Then, the locations $d_{\pm fGP}$ of the center of the integrated spaces can be derived as follows by using the lens equations twice:

$$d_{\pm fGP} = \frac{\pm f_{GP}(g_{GP}(g_{LA} - f_{LA}) - f_{LA}g_{LA})}{g_{GP}(g_{LA} - f_{LA}) - g_{LA}(f_{LA} \pm f_{GP}) \pm f_{LA}f_{GP}} \quad (1)$$

where g_{GP} is the distance from the lens array to the GP lens, and g_{LA} means the gap between the LCD panel and the lens array. Thus, if we set g_{GP} and g_{LA} to 38 mm and 7.4 mm respectively, d_{+fGP} and d_{-fGP} will be 40 mm and 200 mm behind the lens array when the GP lens acts like a convex lens ($+f_{GP} = 100$ mm) and a concave lens ($-f_{GP} = -100$ mm), respectively. The AR images were reflected through a half mirror located 250 mm from the GP lens. Since the distance between the half mirror and the observer was set to be 350 mm, two integrated spaces are formed at 640 mm and 800 mm far from the observer. In addition, two different real objects of a toy car (the 1st object) and a dodecahedron (the 2nd object) were placed also at the locations of those integrated spaces as shown in Fig. 4 in order to verify the locations of the AR images by comparing the focus cues and parallaxes of them. The parameters of experimental setup are listed in Table 1.

3.2 Optimization of APSD Operation

In implementing the time-multiplexing depth-switchable 3D AR system, an accurate synchronization between the time-sequential depth floating of the GP lens by the APSD and the relevant depth image expression by the LCD panel is essential. To achieve that goal, the switching dynamics of the APSD were evaluated by measuring the transmitted intensities through a circular polarizer (the transmission polarization state is RHCP) as an analyzer with a 532 nm CW laser. The temporal transmittance variation was measured by using a photo-diode and an oscilloscope (DSO1052B, KEYSIGHT Ltd.). Figure 5 shows the measurement results of the switching dynamics of the APSD. As shown in Fig. 5(b) and 5(c), the field-on response time, t_{on} ~1.5 ms, (required for the polarization switching from LHCP to RHCP) of the APSD was much faster than the field-off response time, t_{off} ~34.4 ms, (required for the polarization switching from RHCP to LHCP). The reason is that the t_{on} level is determined by the field-induced dielectric torque of the LC molecules, but the t_{off} level is determined by the elastic relaxation of the LC molecules by the surface anchoring effect.

TABLE 1
Experimental Parameters

Pixel pitch of the LCD panel	47 μm
Refresh rate of the LCD panel	50 Hz
Focal length of the lens array (f_{LA})	10 mm
Pitch of the elemental lens	5 mm
Distance from the lens array to the GP lens (g_{GP})	38 mm
Distance from the display device to the lens array (g_{LA})	7.4 mm
Focal length of GP lens (f_{GP})	100 mm
Aperture size of the GP lens (S_{GP})	24.5 mm
Size of the 1st integrated space I_{+fGP}	10 mm
Size of the 2nd integrated space I_{-fGP}	11.7 mm

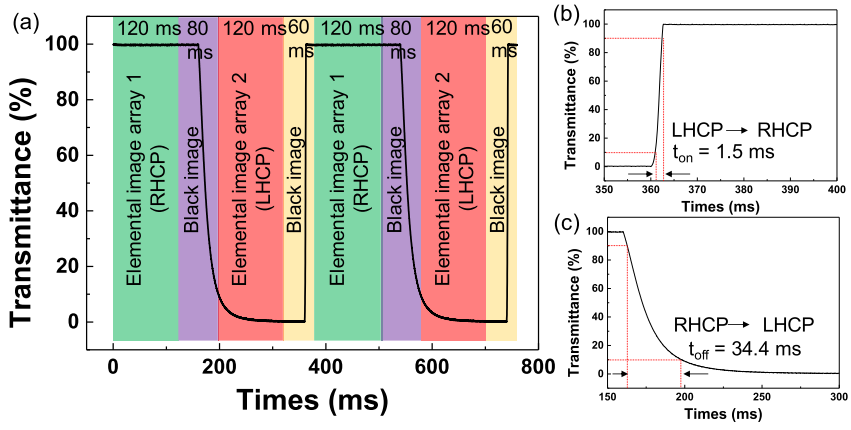

Fig. 5. Switching dynamics of the APSD characterized with a circular polarizer as an analyzer: (a) polarization-switching characteristics of the APSD co-plotted with the corresponding image frame signals, (b) and (c) enlarged results showing the field-on and field-off response properties, respectively.

Considering the asymmetric behavior of the switching dynamics of the APSD and to minimize the crosstalk between the term for the polarization transitions and the elemental switching, black image frames are introduced with different duration times between two elemental image sets to be integrated and floated to the 1st and the 2nd volume spaces. Though the maximum switching rate of the proposed system between the integrated spaces is up to 3 Hz currently and suitable for an application such as a depth-switchable 3D AR system providing near and far integrated spaces in accordance of the locations of environmental objects, we expect that the APSD dynamics can be much improved by employing fast-switching LC modes like optically-compensated bend modes [14]. In this case, a stacked LC structure should be considered to give the wavelength-insensitive polarization switching ability to the APSD [15].

3.3 Analysis of Viewing Parameters

Although there are various studies about the viewing characteristics of the conventional integral floating display, the restriction from the finite aperture of the floating lens for the formation of the viewing region has not been analyzed yet [16], [17]. In this section, we analyze the formation of the viewing region of the proposed system using a floating lens (GP lens) with a finite aperture. Based on Eq. (1), the viewing angle and the formation of the viewing zone depend on the location of the observer. Thus, we added a parameter *D* which means the distance from the GP lens to

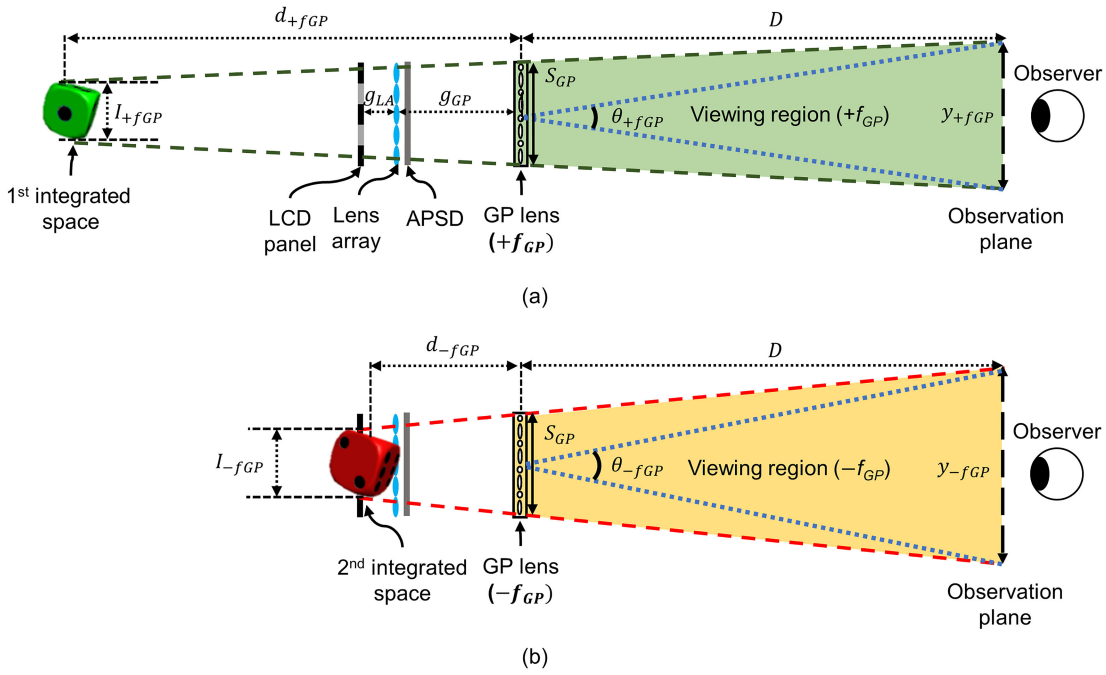

Fig. 6. Viewing parameters of the proposed system when the GP lens acts like (a) a convex lens with $+f_{GP}$, and (b) a concave lens with $-f_{GP}$.

the observer to analyze the viewing angle. Figure 6 shows the formation of the viewing region and corresponded viewing angle when the 1st and the 2nd integrated spaces are reconstructed. From the geometry shown in Fig. 6(a) and 6(b), the lateral size $y_{\pm fGP}$ of the observation plane and the viewing angle of $\theta_{\pm fGP}$ can be derived as follows.

$$y_{\pm fGP} = S_{GP} - D\frac{S_{GP} - I_{\pm fGP}}{d_{\pm fGP}} \tag{2}$$

$$\theta_{\pm fGP} = 2\tan^{-1}\left(\frac{y_{\pm fGP}}{2D}\right) \tag{3}$$

$$FoV_{sys} = 2\tan^{-1}\left(\frac{S_{GP}}{2D}\right) \tag{4}$$

$$FoV_{\pm fGP} = 2\tan^{-1}\left\{\frac{\min\left[S_{GP}, D\left(I_{\pm fGP}/D - d_{\pm fGP}\right)\right]}{2D}\right\} \tag{5}$$

Then, we can expect that the viewing angles of the 1st and 2nd integrated spaces (θ_{+fGP} and θ_{-fGP}) will be about 6° and 20° if $D = 350$ mm + 250 mm = 600 mm as presented at Fig. 4. Due to the finite aperture size S_{GP} of the GP lens, the viewing angle of the farther integrated space (1st integrated space) will be narrower than that of closer one. In addition, the maximum field of view (FoV) of the proposed system (FoV_{sys}) is derived as Eq. (4) from D and S_{GP} and has a value of 2.34° for our experimental setup. We can also calculate the FoV of each integrated space ($FoV_{\pm fGP}$) to be 0.72° and 1.05° using Eq. (5) with the experimental parameters given at Table 1. The 1st integrated space is designed to be a smaller FoV than 2nd one since it is located at farther position and a smaller size. The use of operator 'min[]' to choose lesser value is for preventing a result that the calculated FoV of integrated space exceeds the maximum FoV of the system. As denoted in the eqs. (3) and (5), the aperture size S_{GP} is a main factor to restrict the viewing angle and the FoV of integrated spaces. Thus, we designed the integrated spaces to have a FoV of around

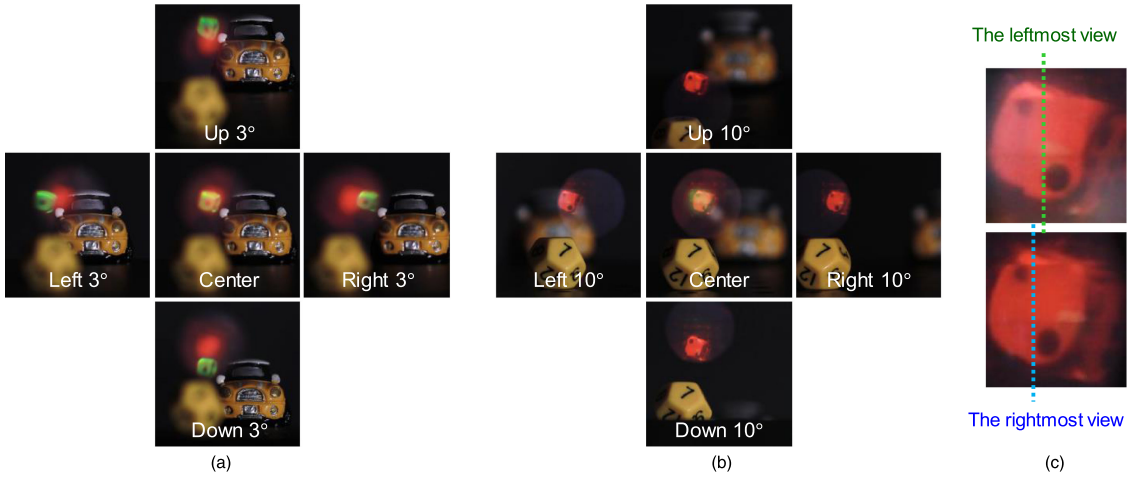

Fig. 7. Verification of accommodation (Visualization 1), and motion parallax of dual volumetric spaces with a focus of capturing device at (a) the 1st object (Visualization 2), (b) the 2nd object (Visualization 3), and (c) comparison of different motion parallaxes of the nearer integrated space at the leftmost/rightmost views.

1° in order to enlarge the viewing angle under that restriction. With the small FoV conditions above, we could observe the floating depth volume images within the viewing angles of 6° and 20° for the nearer and farther integrated spaces as shown in Fig. 6 despite the small S_{GP} condition employed in our experiment. Though we admit that the viewing angles and the FoVs of our experimental demonstration are not satisfactory yet despite the effort above, we expect that they will be improved if a GP lens with a larger aperture (S_{GP}) is implemented for consumer applications.

3.4 Experimental Results and Verification of Integrated Space Locations

The experimental verification has been conducted by checking two 3D cues of accommodation and motion parallax. At first, Visualization 1 shows the change of accommodation cue while changing the focus of capturing device with a lens of 50 mm f/2.5. In the supplement, when the focus of capturing device is at the 1st object (toy car) and 2nd object (dodecahedron), AR images in corresponding integrated spaces are also shown clearly. In the contrary, the object and AR image outside of the depth of focus of the capturing device is shown blurred together. Thus, we can confirm that the cue of accommodation supports that the location of each volumetric space (green die & red die) is matched with that of the corresponding real object (toy car & dodecahedron), respectively.

The next verification is based on the motion parallaxes. In Fig. 7(a), the 1st object (toy car) and the AR image (green die) in the 1st volumetric space show the same motion parallaxes with viewing angle of 6° as expected. The 2nd object (dodecahedron) and the AR image (red die) in the 2nd volumetric space also show the same motion parallax with viewing angle of 20° as shown in Fig. 7(b). Therefore, it can be confirmed that dual integrated spaces are properly realized as designed and the depth range of the integral floating display is much improved than the previous proposals [18]. The 2nd verification is also presented in Visualization 2 and 3 with different focuses of capturing device. For demonstrating full color floating volume images, the chromatic aberration property of the employed GP lens should be essentially considered first [11], [19]. In addition, each color (R/G/B) pixels can be integrated at slightly different depths in order to be combined altogether after floated by a GP lens with pre-consideration on a chromatic aberration of a GP lens, which will be a subject of a further research.

Besides, there is a crosstalk between the integrated spaces from the wavelength-dependent focusing efficiency of the GP lens used in our experimental demonstration [11]. This artifact causes a light leakage to undesignated integrated space and will result a ghost image to degrade the

contrast of 3D images, as shown in the red color image volume of Fig. 7(b) [20]. In order to resolve this issue, the implementation of an achromatic GP lens and locating the integrated spaces farther from the LCD panel are expected to be helpful.

4. Conclusion

In this paper, an augmented-reality (AR) device which presents virtual volumetric images to switchable integrated spaces is proposed and demonstrated. Using the optically anisotropic property of the GP lens, the locations of the AR images with the polarization modulation between RHCP and LHCP can be time-sequentially switched between dual integrated spaces. The experimental results show that the depth range of the volumetric AR images can be increased 160 mm with the adoption of the bi-focal integral floating display. The proposed method is expected to be used for various AR applications owing to its compact form factor and absence of mechanical movement.

References

[1] J.-H. Park and S.-B. Kim, "Optical see-through holographic near-eye-display with eyebox steering and depth of field control," *Opt. Exp.*, vol. 26, no. 21, pp. 27076–27088, 2018.
[2] H.-J. Yeom *et al.*, "3D holographic head mounted display using holographic optical elements with astigmatism aberration compensation," *Opt. Exp.*, vol. 23, no. 25, pp. 32025–32034, 2015.
[3] Y. Takaki and Y. Yamaguchi, "Flat-panel type see-through three-dimensional display based on integral imaging," *Opt. Lett.*, vol. 40, no. 8, pp. 1873–1876, 2015.
[4] Y. Yamaguchi and Y. Takaki, "See-through integral imaging display with background occlusion capability," *Appl. Opt.*, vol. 55, no. 3, pp. A144–A149, 2016.
[5] X. Hu and H. Hua, "High-resolution optical see-through multi-focal-plane head-mounted display using freeform optics," *Opt. Exp.*, vol. 22, no. 11, pp. 13896–13903, 2014.
[6] S. Liu, Y. Li, P. Zhou, S. Huang, Q. Chen, and Y. Su, "A multi-plane optical see-through head mounted display with reverse mode PSLC," in *Proc. SID Int. Symp. Dig. Tech. Papers*, 2017, pp. 763–766.
[7] T. Zhan, Y.-H. Lee, and S.-T. Wu, "High-resolution additive light field near-eye display by switchable Pancharatnam–Berry phase lenses," *Opt. Exp.*, vol. 26, no. 4, pp. 4863–4872, 2018.
[8] G. Tan, T. Zhan, Y.-H. Lee, J. Xiong, and S.-T. Wu, "Polarization-multiplexed multiplane display," *Opt. Lett.*, vol. 43, no. 22, pp. 5651–5654, 2018.
[9] J. Hong, S.-W. Min, and B. Lee, "Integral floating display systems for augmented reality," *Appl. Opt.*, vol. 51, no. 18, pp. 4201–4209, 2012.
[10] H. Hua and B. Javidi, "A 3D integral imaging optical see-through head mounted display," *Opt. Exp.*, vol. 22, no. 11, pp. 13484–13491, 2014.
[11] J. Kim, Y. Li, M. N. Miskiewicz, C. Oh, M. W. Kudenov, and M. J. Escuti, "Fabrication of ideal geometric-phase holograms with arbitrary wavefronts," *Optica*, vol. 2, no. 11, pp. 958–964, 2015.
[12] T. Zhan *et.al.*, "Pancharatnam–Berry optical elements for head-up and near-eye displays," *J. Opt. Soc. Amer. B, Opt. Phys.*, vol. 36, no. 5, pp. D52–D65, 2019.
[13] D.-K. Yang and S.-T. Wu, *Fundamentals of Liquid Crystal Devices*. New York, NY, USA: Wiley, 2006.
[14] S.-G. Kang, J.-S. Lee, H.-H. hwang, and C.-S. Cho, "P-78: A design optimization of the OCB-mode for the application of field-sequential color microdisplays," in *Proc. SID Int. Symp. Dig. Tech. Papers*, 2001, pp. 855–857.
[15] M. D. Lavrentovich, T. A. Sergan, and J. R. Kelly, "Switchable broadband achromatic half-wave plate with nematic liquid crystals," *Opt. Lett.*, vol. 29, no. 12, pp. 1411–1413, 2004.
[16] J. Yim, Y. Kim, and S.-W. Min, "Analysis on image expressible region of integral floating," *Appl. Opt.*, vol. 55, no. 3, pp. A122–D126, 2016.
[17] J. Kim, S.-W. Min, Y. Kim, and B. Lee, "Analysis on viewing characteristics of an integral floating system," *Appl. Opt.*, vol. 47, no. 19, pp. D80–D86, 2008.
[18] S.-W. Min, J. Kim, and B. Lee, "New characteristic equation of three-dimensional integral imaging system and its applications," *Jpn. J. Appl. Phys.*, vol. 44, no. 2, pp. L71–L74, 2005.
[19] C. Yousefzadeh, A. Jamali, C. McGinty, and P. J. Bos, "'Achromatic limits' of Pancharatnam phase lenses," *Appl. Opt.*, vol. 57, no. 5, pp. 1151–1158, 2018.
[20] S. Shestak, D. Kim, and S. Hwang, "Measuring of gray-to-gray crosstalk in a LCD based time-sequential stereoscopic display," in *Proc. SID Int. Symp. Dig. Tech. Papers*, 2010, pp. 132–135.